

NUMERICAL SIMULATIONS OF DYNAMIC FRACTURE. CRACK PROPAGATION AND FRACTURE OF INITIALLY INTACT MEDIA

V. Bratov^{1,2*}

¹Institute for Problems in Mechanical Engineering, Russian Academy of Sciences, St. Petersburg 199178, Russia

²Peter the Great St. Petersburg Polytechnic University, St. Petersburg 195251, Russia

*e-mail: vladimir@bratov.com

Abstract. The paper briefly reviews progress in numerical simulations of dynamic crack propagation and fracture of initially intact media and presents examples of simulations utilizing finite element method with embedded dynamic fracture criterion based on the concept of incubation time of brittle fracture introduced by Petrov and Morozov. The examples include dynamic fracture initiation, propagation arrest, and evolution of fracture zones in initially intact media. It is demonstrated that this approach is capable to give an accurate description of all the variety of phenomena associated with dynamic fracture. An important feature of the approach, distinguishing it from the majority of other dynamic fracture criteria is the necessity to introduce but one additional material parameter, easily evaluated experimentally, in order to predict dynamic fracture.

Keywords: FEM, dynamics, fracture, incubation time, crack velocity, crack arrest, quasibrittle fracture, erosion

1. Introduction

First experimental results in dynamic fracture are dating back to the beginning of the 20th century (see ex. [1-4]). The interest in the area was primarily driven by military applications – i.e., the development of protection systems to protect humans and structures against high-energy impacts and the development of new weapons to penetrate this protection. First theoretical results for cracks propagating with velocities comparable to that of the Rayleigh wave appeared in the middle of the 20th century ([5-7]) along with the progress in linear elastic fracture mechanics (LEFM).

Later on, in the 1970s and 1980s experimental dynamic fracture mechanics got additional attention due to new emerging applications in such areas as high-speed transportation systems, aerospace applications, micromechanics, nuclear safety, etc. and the appearance of accurate high temporal resolution experimental techniques that made it possible to capture the evolution of fracture on micro- and nano-second time scale (see ex. [8-18]). Most of the analytical solutions for dynamic crack propagation known to date had also appeared at about the same time [19-27,35].

Despite the significant interest caused by very important and topical applications, long history of investigations, and certain progress in the area, to the moment there is no generally accepted approach for simulation of dynamic fracture initiation and evolution in quasibrittle materials. The difficulties are primarily caused by complicated and expensive experiments requiring very precise loading techniques and extremely sensitive high temporal resolution equipment for registration of dynamic fracture evolution.

2. Fracture criterion

The central difficulty associated with analytical and numerical simulations of dynamic crack propagation is the choice of criterion for crack initiation, propagation, and arrest. In early attempts, authors were trying to utilize the critical stress intensity factor criterion, which was extremely successful for the prediction of fracture onset in quasistatic conditions. Very soon numerous experimental results (see ex. [12,15,16]) explicitly demonstrated that stress intensity factor, controlling the stress field surrounding the crack tip, at the instant of crack initiation is extremely unstable. It was observed that for the same quasibrittle material, the dynamic critical stress intensity factor (the value of stress intensity factor at the instant of fracture onset) can take a rather arbitrary value depending on experimental conditions. This value can both exceed and be smaller than the critical stress intensity factor value typical for quasistatic conditions.

Following attempts, originating from the works of Freund [19-21] and later developed by Rosakis were based on an assumption that dynamic critical stress intensity factor can be defined as a function of stress intensity rate. Though this approach can be applied for the prediction of fracture initiation for some materials (usually displaying a well-developed plastic zone at the tip of a crack) in a rather limited range of experimental conditions, new experimental results (see ex. [28]) had shown that dynamic critical stress intensity factor cannot be treated as a fractured material property, being strongly dependent on experimental geometry and loading conditions. Moreover, multiple publications (ex. [16]) clearly demonstrated that in some cases fracture at the crack tip can be initiated at the instant when the stress intensity factor rate is negative (also see discussion in [29]). Obviously, the abovementioned experimental results testify inapplicability of the rate-dependent critical dynamic stress intensity factor criterion to serve as a universal crack initiation or propagation criterion.

Another criterion, that can be utilized to determine critical conditions leading to crack initiation and arrest was proposed by Petrov and Morozov [29,30]. The criterion is based on the concept of incubation time of essentially transient process of brittle fracture. As demonstrated in multiple publications (ex. [31-34,36,37]), this approach can successfully predict all the variety of experimentally observed phenomena associated with the dynamic fracture of quasibrittle media. The incubation time fracture criterion will be introduced in section 4. Several solutions received utilizing the incubation time approach embedded into the finite element method (FEM) will be presented. An important feature of this approach is the necessity to introduce but one material parameter in addition to standard material strength parameters. This parameter – incubation time of brittle fracture has an explicit physical meaning and can rather easily be evaluated experimentally.

The last group of approaches that can be utilized in order to predict crack initiation and propagation in dynamic conditions are criteria based on equations of state for material (ex. [38]) or equations of state for a cohesive zone (ex. [39,42]), placed on the crack path or equations for interaction between discrete particles representing the material (ex. [40]). When such equations of state are introduced, the fracture criterion is received as critical separation or critical crack opening, etc. A common disadvantage of this approach is the necessity to introduce and identify a big number (in some cases up to 15) of material parameters that often have no explicit physical meaning and comprehensible experimental technique to evaluate. In most cases, the parameters are evaluated by fitting theoretical prediction or numerical realization to experimental observations. As a result, in most cases, the received model is only applicable for simulation of the experimental conditions used for parameter identification. For many of these methods sensitivity to discretization, size is also a significant problem.

Here one can also mention different variations of phase-field models (PFM's) (see ex. [41]). PFM's are coupling regularized variational formulation of fracture condition and

material damage models. Although this approach, being the direct generalization of Griffith's brittle fracture theory is properly physically reasoned, the problem of parameter identification is greatly limiting the predictive ability of the solutions.

3. Numerical techniques for dynamic cracks

As discussed in the previous section for simulations of dynamic crack propagation the utilized fracture condition is of major significance. The numerical scheme used for integration of media equations of motion is phenomenologically not that much important and mainly affects the computational cost to solution accuracy ratio. Different approaches can be more or less efficient and convenient for the creation of a new surface (i.e., crack propagation), but again, if applied correctly, utilizing different approaches sharing the same fracture criterion, should not lead to substantially different computational results.

One of the most widely used methods to solve equations of motion for solid media is the finite element method (FEM). FEM is also the most utilized method for simulations in wave mechanics, including dynamic fracture mechanics. FEM utilizing explicit or implicit time integration is often employed to solve linear (suitable for many problems implying quasibrittle fracture) problem of dynamic elasticity while nonlinearity is introduced by the change in the boundary following the execution of fracture criterion. Examples presented in the following sections of this paper were received utilizing commercial FEM software (ANSYS, ABAQUS, and LS-DYNA) with incubation time fracture criterion embedded into this software. In some cases, execution of the fracture criterion was controlled by external software while FEM software was only used to receive solution for displacement field on every time integration substep.

An interesting and very promising approach for both quasistatic and dynamic fracture mechanics is the extended finite element method (XFEM) (see ex. [43]) extension of FEM. XFEM, through the partition of unity concept, is locally enriching finite elements enabling a possibility to have either discontinuity on an interface cutting finite element or singularity inside. This extension provides a very simple instrument for crack propagation, leading to converging solutions without a necessity to modify mesh once the fracture geometry is changed. XFEM can also be utilized in combination with the spectral element method (SEM) (ex. [44]), giving a possibility to receive accurate solutions on a much coarser mesh. The concept of level-sets is also widely used to describe crack paths (see ex. [45]).

Many other methods, suitable for solving partial derivative equations (PDE's) of media motion or reformulations of these equations can be utilized for the simulation of dynamic crack propagation. Peridynamics (see ex. [46]), reformulating PDE's of classical elasticity as integral equations are particularly suitable for fracture mechanics and dynamic fracture mechanics removing difficulties connected with derivatives on boundaries and singularities. Different discrete element methods (DEM's) including molecular dynamics (MD) in some cases can provide a deeper understanding of physical mechanisms underlying dynamic fracture at the crack tip (see ex. [47]). Due to computational cost limitations on dimensions of a domain that can be simulated, it is also possible to couple DEM, solving the problem at the vicinity of the crack tip with other approaches (FEM, SEM, XFEM, etc.) providing a solution elsewhere within the solution domain (see ex. [48]).

4. Incubation time fracture criterion

Incubation time criterion for brittle fracture at a point x at time t reads (see ex. [29,30]):

$$\frac{1}{\tau} \int_{t-\tau}^t \frac{1}{d} \int_{x-d}^x \sigma(x', t') dx' dt' \geq \sigma_c, \quad (1)$$

where τ is the incubation time of a brittle fracture process – a parameter characterizing the response of fractured material microstructure to changing transient force field. τ is constant for a given material at a given scale level. Its value does not depend on the problem geometry,

neither it depends on the way a load is applied nor on the shape of a load pulse and its amplitude. d is the characteristic size of the fracture process zone. Its value is constant for a given material at a given scale level. σ is normal stress at a point, changing with time and σ_c is its critical value (ultimate stress or critical tensile stress evaluated in quasistatic conditions). x' and t' are the local coordinate and time.

Assuming

$$d = \frac{2 K_{IC}^2}{\pi \sigma_c^2}, \quad (2)$$

with K_{IC} being the critical value of stress intensity factor for mode I loading (mode I fracture toughness), measured in quasistatic experimental conditions, it can easily be shown that within the framework of linear elastic fracture mechanics for the case of fracture initiation in the tip of an existing crack, (1) is equivalent to:

$$\frac{1}{\tau} \int_{t-\tau}^t K_I(t') dt' \geq K_{IC}. \quad (3)$$

Condition (2) naturally arises from the requirement that (1) is equivalent to Irwin's fracture criterion ($K_I \geq K_{IC}$), in quasistatic conditions or, which is the same, for $t \rightarrow \infty$. In other words, such a choice of d guarantees that for slow loading rates and, hence, times to fracture that are significantly greater than τ , condition (3) for crack initiation gives the same predictions as Irwin's criterion of a critical stress intensity factor. In the case when the stress field is not singular in the vicinity of point x (locally intact material) and under the condition of quasistatic load applied to the media, condition (1) is reduced to a critical tensile stress fracture criterion ($\sigma \geq \sigma_c$).

Within the framework of the incubation time approach, linear size d , formally introduced as a requirement that condition (1) coincides with critical stress intensity factor criterion for quasistatic situation, has a much deeper physical meaning. d is giving a minimal rupture size that can be called *fracture* on a chosen scale level. Thus, d is giving a dimension for scale level – any defect with a linear size substantially smaller than d is not treated as fracture and material is locally intact. This idea is of special importance for numerical analysis: the choice of rupture surface increment once fracture condition is executed somewhere in the body is a common difficulty for numerical schemes employing time discretization. For many of the known numerical approaches in dynamic fracture, the choice of fracture increment per time step is known to significantly affect the received fracture evolution history. Adopting linear size d to be the unit fracture length (on a given scale level) removes this difficulty – once fracture condition is executed somewhere in the body, a new surface with a length of d should appear in the vicinity of this point. In the following sections, it will be demonstrated that the described approach is capable of very precise description and prediction of dynamic crack evolution in quasibrittle materials. The very important feature of this approach, distinguishing that from the majority of other known approaches in dynamic fracture, is the necessity to introduce a single parameter in addition to standard traditionally utilized material strength parameters – incubation time τ . The value τ can be rather easily evaluated experimentally (see ex. [29,30]). A very limited set of material properties- elastic properties (Young's modulus, Poisson's ratio, density), quasistatic strength properties (ultimate strength, critical stress intensity factor), and dynamic strength property (incubation time of brittle fracture) is providing a possibility to simulate all the variety of known experimental results for quasibrittle dynamic fracture.

This approach was embedded into commercial FEM computational software (ANSYS, ABAQUS, and LS-DYNA). This paper will present results of simulations in comparison to experimental measurements for evolution (initiation, propagation, arrest, reinitiation) of preexisting cracks as well as the results of incubation time approach simulations in comparison to experiments for fracture of initially intact media subjected to high-energy high-velocity dynamic impact.

5. Initiation, propagation, arrest, and reinitiation of dynamic cracks

In [50] the described above approach was applied to simulate conditions of classical for fracture dynamics experiments of Ravi-Chandar and Knauss [11]. In these experiments cracked samples made of Homolite-100 (transparent organic glass) were subjected to the pulsed dynamic load applied at the existing crack faces. The load was created by the magnetic field created between two flat conductors inserted into the crack. A sketch of the experimental geometry is given in Fig. 1.

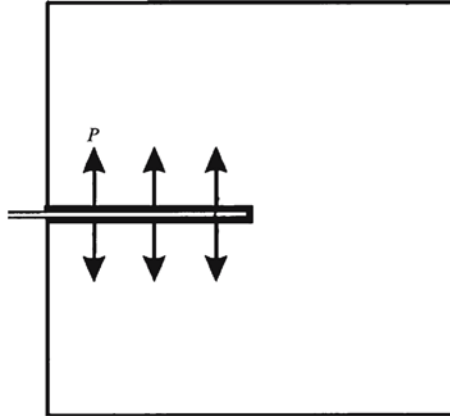


Fig. 1. Experimental geometry used in [11]

Utilized electromagnetic loading gives the pressure that is uniformly distributed over the crack faces with an intensity that is directly proportional to the current in the circuit. The current in the circuit can easily be measured in the experiment. The temporal shape of the loading pulse, created in [11] is presented in Fig. 2.

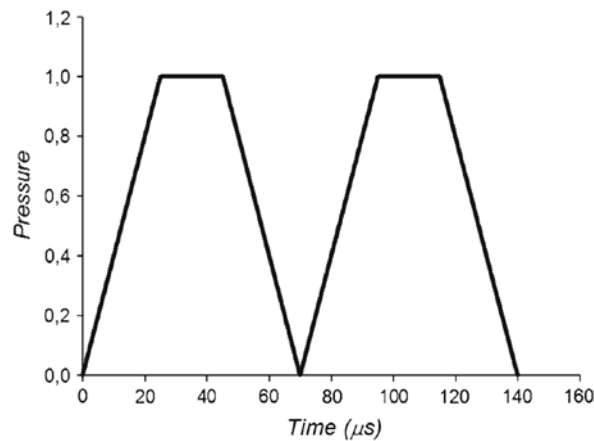


Fig. 2. Temporal shape of the load created in [11]

Such a load shape (two consequently following pulses) results in the initiation of fracture in the tip of the existing crack followed by crack propagation (at almost constant velocity), crack arrest, and reinitiation when the second pulse is coming into the play. Experimentally measured crack extension history is given in Fig. 3.

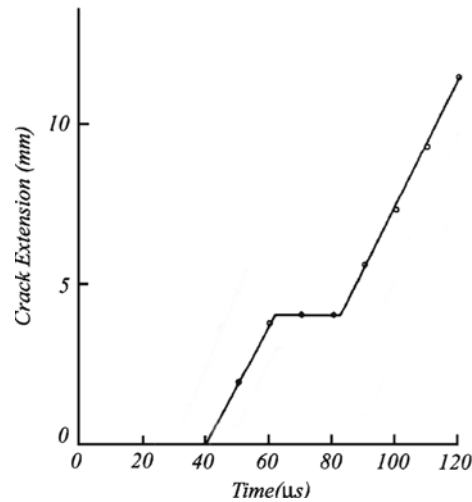


Fig. 3. Crack extension history observed in [11]

Utilizing the described above incubation time criterion for brittle fracture, embedded into ANSYS FEM [51] commercial software, the exact conditions of experiments [11] were simulated. Material (Homolite-100) properties used for simulations are given in Table 1.

Table 1. Homolite-100 properties used for numerical simulations

Density	ρ , kg/m ³	1230
Young's modulus	E, MPa	3900
Poisson's ratio	ν	0.35
Critical stress intensity factor	K_{IC} , MPa \sqrt{m}	0.48
Ultimate tensile strength	σ_C , MPa	48
Incubation time of brittle fracture	τ , μ s	9*

*Value for incubation time for Homolite-100 measured in [52]

Standard properties for Homolite-100 presented in Table 1 are taken from the official material datasheet. Value for an incubation time of brittle fracture for Homolite-100 was experimentally evaluated in [52] and was not anyhow fitted within the presented simulations. Due to the problem symmetry (and according to experimental observations), fracture propagates along with the initial crack continuation. Thus, the execution of condition (1) was only controlled along this line. Once the fracture condition is executed in the tip of the crack, the crack length is advanced by d (calculated according to (2), utilizing the node release technique. The model was checked for convergence. It should be highlighted, that the model contains no "tuning" parameters – real experimental conditions (including geometry and boundary conditions) were used for simulations and all of the utilized material parameters are presented in Table 1.

Figure 4 presents the received crack extension history in comparison to experimental measurements (Fig. 3).

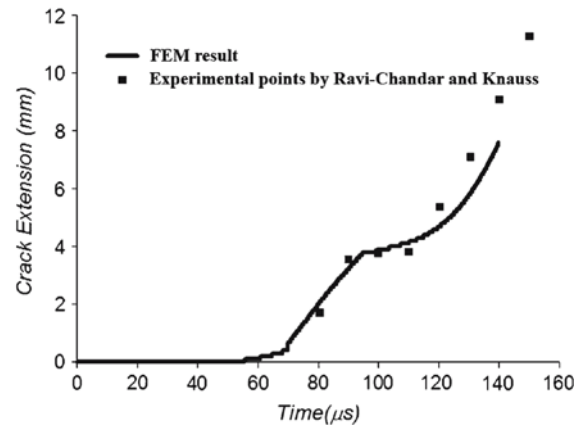


Fig. 4. Calculated crack extension history compared to experimental data from [11]

As follows from the presented computational results, the utilized numerical model is capable of very precise prediction of crack initiation, growth, arrest, and reinitiation. As shown in multiple publications (see ex. [33]), the developed approach provides the correct prediction of crack evolution in different materials under various loading conditions.

6. Stress intensity factor – crack speed relation

Straightforward analysis based on LEFM implies direct relation between the crack tip stress intensity factor (or, which is the same, energy flux into the crack tip) and the crack propagation velocity.

In [11] authors also had a possibility to measure stress intensity factor history utilizing the optical method. Figure 5 gives a history of the stress intensity factor in the crack tip measured in the experiment modeled in the previous section.

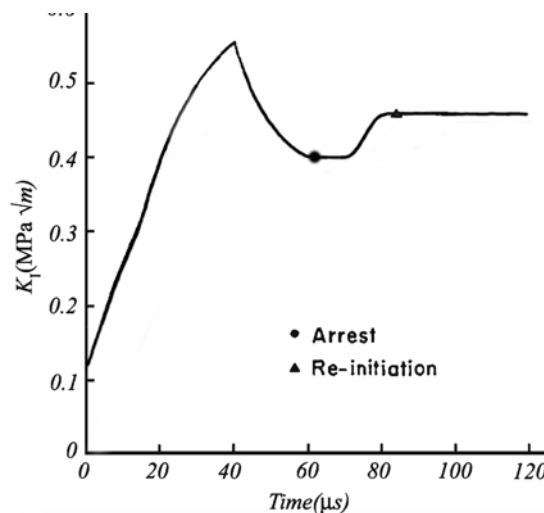


Fig. 5. Stress intensity factor history observed in [11]

As follows from Fig. 3, giving crack extension history and Fig. 5, giving the corresponding stress intensity factor history, the crack, after its first initiation and up to the moment of arrest, is moving with constant velocity whilst the magnitude of the stress intensity factor is changing significantly (from $0.6 \text{ MPa}\sqrt{m}$ to $0.4 \text{ MPa}\sqrt{m}$). Exactly the same behavior is received in the presented above numerical simulation – the crack is propagating at a constant velocity (that is sometimes called ballistic behavior) while the value of the stress intensity factor is vastly changing. A similar effect is observed in a number of experimental

works (see ex. [53]) – dynamic cracks propagate at a constant velocity, exhibiting no relation between stress intensity factor at the crack tip and crack velocity.

Obviously, this behavior contradicts mentioned above direct correlation between the stress intensity factor and the crack speed. At the same time, in other experiments (see ex. [54,55]) authors explicitly observe crack velocity that is in direct relation to the instantaneous value of the stress intensity factor. The presented above numerical approach was applied [56] to simulate the conditions of experiments from [54] in order to see what prediction the incubation time fracture criterion will give in experimental conditions leading to crack speed being directly related to the stress intensity factor value. In these experiments [54] cracked sample was loaded by slow quasistatic load (see Fig. 6) up to the moment of crack initiation. Due to experimental geometry, crack extension results in a significant increase in the crack tip stress intensity factor.

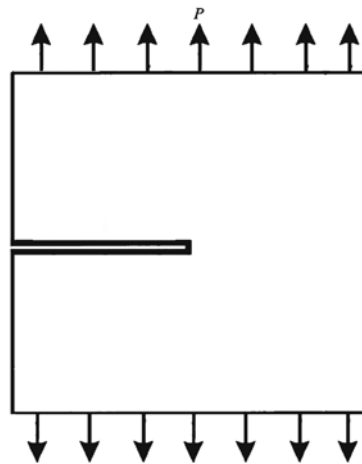


Fig. 6. Experimental geometry used in [54]

All of the experimental conditions from [54], including experimental geometry and boundary conditions, were used for the development of the numerical model. The sample was made of PMMA with the properties presented in Table 2.

Table 2. PMMA properties used for numerical simulations

Density	ρ , kg/m ³	1200
Young's modulus	E, MPa	3500
Poisson's ratio	ν	0.32
Critical stress intensity factor	K_{IC} , MPa \sqrt{m}	1.1
Ultimate tensile strength	σ_C , MPa	60
Incubation time of brittle fracture	τ , μs	1.5*

*Value for incubation time for PMMA measured in [53]

Figure 7 gives a comparison of experimentally measured and numerically evaluated crack velocity plotted against the crack extension.

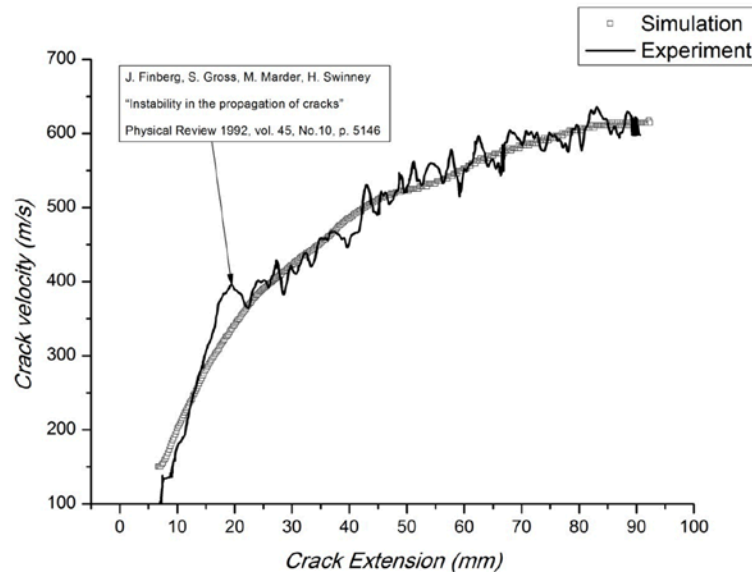


Fig. 7. Experimental geometry used in [54]

As follows from Fig.7 the utilized numerical approach is giving a prediction of crack velocity as a function of crack extension (with the crack extension being directly proportional to stress intensity factor) that is precisely following the experimental measurement. The presented data also means that within the framework of the utilized numerical approach in the simulated experimental conditions there is a connection between the crack velocity and the stress intensity factor.

Another important physical phenomenon is associated with the maximum possible crack velocity. Based on the assumptions of LEFM, for mode I crack, the maximum possible crack speed is limited by the Rayleigh wave speed [57-59]. The reason for that is the limitation on energy transport speed, which, close to solid body boundary, is mostly carried out by Rayleigh waves (see ex. [60]). At the same time, experimentally observed maximum crack speeds rarely exceed 0.7 of that of the Rayleigh wave (see ex. [61]). Crack bifurcation and crack propagation mode change, resulting in the appearance of crack path fractality is believed to be the reason for that (see ex. [62]). The incubation time approach can also be utilized in order to investigate the phenomenon.

7. Fracture in a tip of a crack vs fracture of intact media

Traditionally, starting from quasistatic fracture mechanics approaches predicting fracture of initially intact media (i.e., without significant stress concentrators) and approaches predicting fracture in the tip of an existing macroscopic crack were developing independently. The approaches predicting fracture of nominally defectless media are usually based on the critical value of normal stress, whilst fracture in the crack tip is traditionally assessed based on Griffith [63] - Irwine [64] approach of critical stress intensity factor. Even though physical mechanisms driving fracture in the two cases are obviously the same (as fracture of initially intact media is initiated on microscopic defects, forming local stress concentration), fracture mechanics for bodies with stress concentrators and approaches to fracture in the case of bodies without macroscopic cracks are still existing and developing independently. The same, to a large extent, is true referring to the simulation of dynamic fracture.

At the same time, since many decades ago there had existed an approach that is capable of predicting both the fracture of bodies without stress concentration and fracture at a tip of a macroscopic crack. The approach is named after Heinz Neuber [65,66] and Valentin Novozhilov [67]. The main idea of the approach consists in the assessment of integral force

field intensity at a vicinity of a studied point rather than the value of force field intensity at the point itself. Following this idea, fracture criterion for the quasistatic case can be derived as:

$$\int_{x-d}^x \sigma(x') dx' \geq \sigma_c d, \quad (4)$$

with σ_c being the ultimate stress, x being the point where the fracture is assessed, $\sigma(x)$ giving the local intensity of the normal stress field, and d giving a linear size of a domain surrounding the point x . It is easy to show (see ex. [29]) that should x be the crack tip and should square root singularity control the stress field surrounding this crack tip (i.e., should the stress field be K_I dominated), (4) is equivalent to Griffith-Irwin critical stress intensity factor fracture criterion ($K_I \leq K_{IC}$) [63,64] if d is chosen such that $d = \frac{2 K_{IC}^2}{\pi \sigma_c^2}$, with K_{IC} being

the critical stress intensity factor value. It is also obvious that if the stress field is not changing significantly within $\{x, x+d\}$, then (1) is equivalent to the critical normal stress approach ($\sigma \leq \sigma_c$). In other words, (4) is completely equivalent to the critical normal stress criterion for points without stress singularity and completely equivalent to the Irwin critical stress intensity factor criterion in the case of square root singular crack tip field. For intermediate situations (ex. for singular fields with non-square root singularities – for example for angular notches or for strongly gradient stress fields) (4) will also predict material strength. For example, in [37] Neuber-Novozhilov criterion is utilized to predict fracture and its direction at a tip of inclined crack subjected to the combination of compressive and shear loading.

Utilization of the Neuber-Novozhilov approach gives a possibility to successfully predict both the fracture at the tip of a crack and the fracture at a point without stress singularity within the framework of a unified approach. This possibility is of particular importance for numerical approaches – in order to assess fracture, there is no need to distinguish between points with stress singularity and points without singularity – the same fracture criterion can be used for any point within a body.

Referring to fracture in dynamic situation, the incubation time fracture criterion introduced by Petrov and Morozov (1) is the generalization of the Neuber-Novozhilov approach for dynamic cases. This paper will present several examples of (1) being utilized as fracture conditions embedded into FEM computational scheme to simulate fracture evolution at initially intact media. Dynamic fracture of initially intact media is usually caused by high-velocity contact interaction between two or more bodies. Development of fracture zone is in most cases caused either by intensive shock waves close to contact surface or by compression waves reflected from free boundaries and transformed into tension waves (that is usually referred to as spallation).

The overwhelming majority of known numerical approaches for simulation of fracture evolution in initially intact media are based on the introduction of rather complex equations of state for material (ex. [68]) or introduction of complex cohesive law controlling the separation between discrete subdomains on the body (ex. [69,70]). The biggest disadvantage of both the first group of approaches (ex. Johnson-Cook model, Johnson-Holmquist model, Johnson-Holmquist-2 model, etc.) and the second group of approaches (discrete element method, particle dynamics, peridynamics, etc.) is the necessity to introduce and identify a big number (in some cases up to 15) of material parameters that often have to explicit physical meaning and comprehensible experimental technique to evaluate. In most cases, the parameters are evaluated by fitting theoretical prediction or numerical realization to experimental observations. As a result, in most cases, the received model is only applicable for simulation of the experimental conditions used for parameter identification. For many of these methods sensitivity to discretization, size is also a significant problem. The central issue, distinguishing dynamic fracture processes from the fracture in the quasistatic situation is the transport of energy to and from the fracture zone. For intact media, this energy is transported

within a solid body primarily by bulk waves, whilst close to boundaries, cracks, interfaces, etc., this energy is mostly transferred taking the use of Rayleigh waves [60].

Unlike the majority of other approaches, in order to utilize the Petrov-Morozov incubation time approach (2), it is necessary to introduce a single material parameter in addition to standard material strength parameters. This parameter – incubation time of brittle fracture has an explicit physical meaning and can rather easily be evaluated experimentally (see ex. [30]).

8. Numerical implementation for arbitrary fracture

The finite element method (FEM) [51] is utilized to solve the linear elastic problem for the propagation of waves within fractured solid media. Once fracture criterion (1) is executed somewhere within the body, the fracture should happen and a new surface should appear. The traditional method to create a new surface in FEM is associated with node separation techniques. This approach is convenient in many cases. However, it is associated with rather time-consuming procedures of remeshing and recalculation of displacements, strains, and velocities for the updated mesh. To achieve accurate integration in (1), it is necessary to use small time steps. Having that in mind node separation technique does not look to be the best solution. In the method employed in this study, the finite elements representing the fractured media initially have no common nodes. Before the fracture instant, the degrees of freedom of nodes located at the same position are coupled (Fig. 8). In this case, the FEM solution of the problem coincides with that for the elements sharing common nodes. If the fracture condition is executed in the corresponding node, the limitation on the degrees of freedom is removed and a new surface is formed. The size of each element is exactly equal to the value of d ($d = \frac{2 K_{IC}^2}{\pi \sigma_c^2}$). Such a choice of the finite element size is ensuring that once the fracture condition is executed somewhere in the body, the created rupture size will be equal to d (see section 4 for discussion of fracture increment size once the fracture condition is executed).

Such a choice of element size is also providing a possibility to rewrite (1) as:

$$\frac{1}{\tau} \int_{t-\tau}^t \sigma(t') dt' \geq \sigma_c, \quad (5)$$

with i assuming values 1 and 2. Repeating indices do not dictate summation in this case. Spatial integration is removed because the stress in the respective direction calculated by FEM software is already giving a mean stress value over the interval equal to d (since d is the element size being used). If (5) is executed for σ_{11} and σ_{22} then restrictions on displacements of nodes 1,2,3 and 4 on Fig. 8 are removed. If (5) is executed for σ_{11} , two new couple sets consisting of nodes 1,2, and 3,4 are created. If (5) is executed for σ_{22} , new couple sets are created for nodes 1,3, and 2,4. For later times condition (5) in the applicable direction is checked for the newly created couple sets separately. Contact between fragments detached from the main body can be simulated or the effect of these fragments on the later fracture evolution can be neglected.

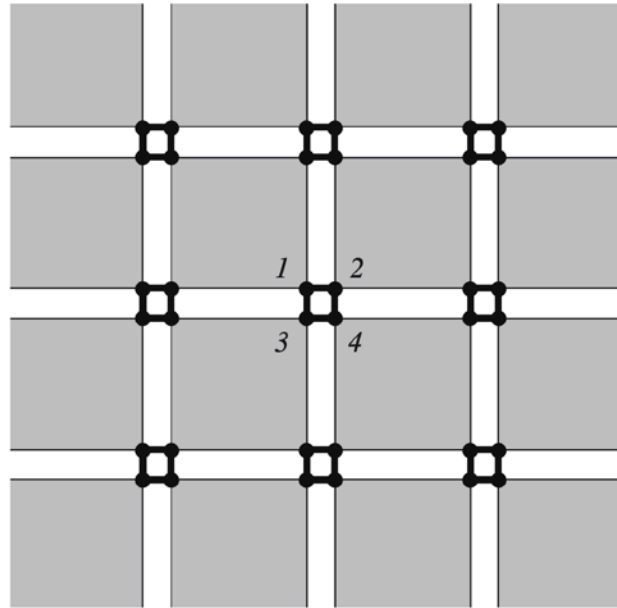


Fig. 8. Finite element model with elements having no common nodes

9. Impact crater formation

The presented above approach was applied to simulate conditions of SMART-1 satellite impacting the surface of the Moon. Year 2006 European Space Agency (ESA) deliberately directed SMART-1 satellite to impact the surface of the Moon [71,72]. The main reason was to study the cloud of dust and debris created by the impact, but the dimensions of the created imprint (crater) were also measured. The contact of the satellite with the lunar surface took place at a velocity of about 2000 km/s; the satellite had a shape close to cubic with a characteristic size of ~1 m and a mass of 366 kg. The observed defect (crater) formed on the Moon's surface as a result of the impact was about 6–10 m in diameter and 3 m deep. The purpose of the presented investigation was to compare the actual sizes of the created crater with the fracture dimensions obtained in simulations of the impact by the FEM scheme incorporating the fracture incubation time criterion.

Properties for the Moon material were taken to be equal to the properties of earth basalt (see Table 3).

Table 3. Moon material properties used for numerical simulations

Density	ρ , kg/m ³	2850
Young's modulus	E, GPa	60
Poisson's ratio	ν	0.25
Critical stress intensity factor	K_{IC} , MPa \sqrt{m}	2.94
Ultimate tensile strength	σ_C , MPa	10.5
Incubation time of brittle fracture	τ , μs	80*

*Value for incubation time for earth basalt from [49]

Value for an incubation time of brittle fracture for the material presenting the Moon was not anyhow fitted within the presented simulations. The rest of the material properties are standard handbook properties for basalt.

Contact interaction was simulated for a cylinder having 1 m in diameter and 1 m in height impacting half-space at a velocity of 2000 m/s. The cylinder material density was chosen such that the projectile's total mass is 366 kg. Equations of dynamic linear elasticity were solved utilizing ANSYS [51] commercial FEM software. Execution of condition (5) at all of the nodes representing half-space was controlled by ANSYS ADPL subroutine.

Figure 9 highlights nodes of the material representing the Moon for which fracture criterion (5) was executed during simulation.

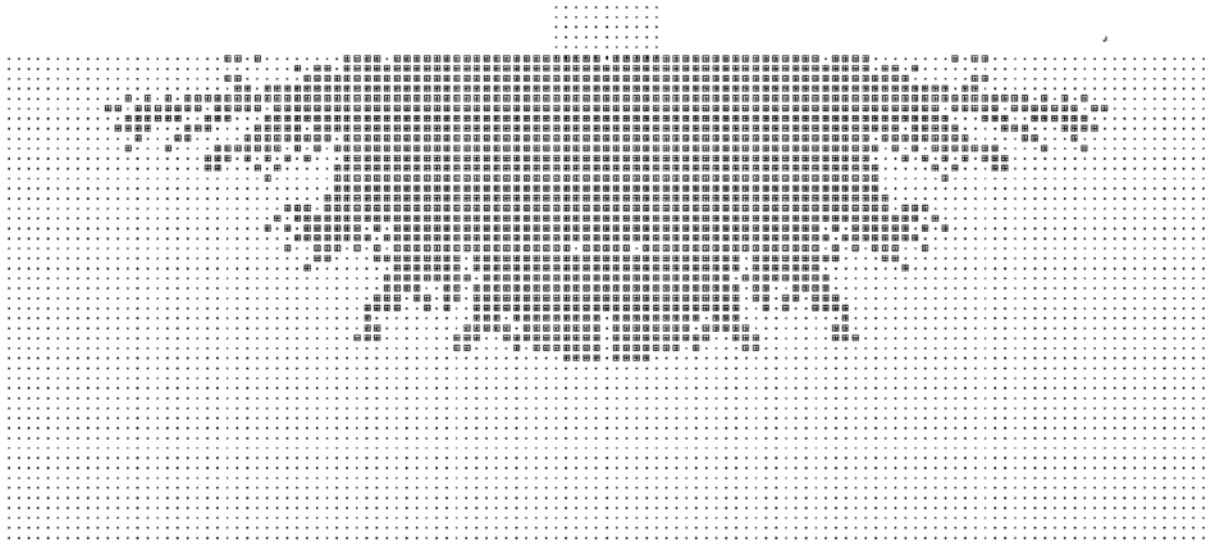


Fig. 9. Nodes representing the Moon where fracture criterion was executed

Thus, it is possible to estimate the dimensions of the imprint (crater) formed as a result of the SMART-1 impact on the Moon's surface. The received damaged zone is about 10 m in diameter and approximately 3 m deep. The region of complete fragmentation of the material can be estimated to be 7-10 m in diameter and 3 m deep. These results perfectly coincide with the dimensions of the crater as estimated by the ESA [71, 72].

10. Ballistic impact

In [31] ballistic impacts of PMMA plates of several different thicknesses were studied experimentally and numerically. As a result of this study, it was clearly demonstrated that the incubation time approach employed to simulate 3D problem of high-speed contact interaction between an impactor and a plate of quasibrittle material can robustly predict both the ballistic limit and residual impactor velocity for initial impactor velocities above the ballistic limit. Here the main results of this study will be presented.

Experimental studies were conducted utilizing a light gas gun capable of accelerating cylindrical impactors made of steel to various velocities. Steel cylinders were normally impacting PMMA plates of three different thicknesses. High-speed photography was employed to register the initial (prior to contact with PMMA plate) and residual velocity of the impactor. As a result of the experimental study, residual velocity was measured as a function of initial velocity for the three studied plate thicknesses – 4mm, 6mm, and 10mm.

The exact conditions of this experiment were simulated utilizing LS-DYNA FEM commercial software with embedded incubation time fracture criterion. In this case, the full 3D problem was solved. Element death technique was utilized in order to simulate fracture once fracture criterion is executed at some location within the PMMA sample. Figure 10 gives the initial problem geometry and FEM mesh.

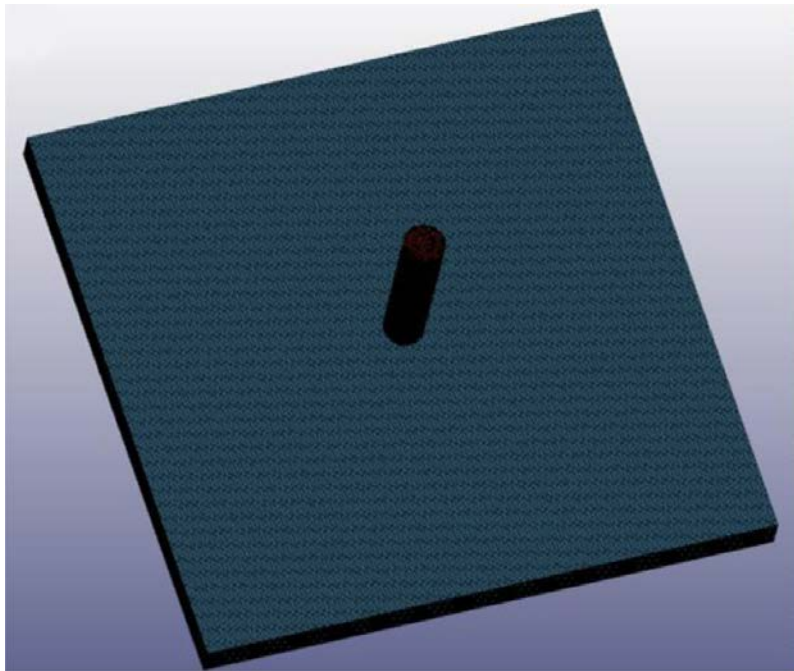


Fig. 10. Problem geometry (6mm thick PMMA plate) and FE mesh

Material properties utilized for simulation are given in Table 4.

Table 4. PMMA properties used for numerical simulations

Density	$\rho, \text{kg/m}^3$	1180
Young's modulus	E, MPa	3300
Poisson's ratio	ν	0.35
Critical stress intensity factor	$K_{IC}, \text{MPa}\sqrt{\text{m}}$	1.7
Ultimate tensile strength	σ_C, MPa	72
Incubation time of brittle fracture	$\tau, \mu\text{s}$	1*

*Value for incubation time for PMMA measured in [24]

Properties for impactors were taken to be equal to the ones typical for steel. Figure 11 gives the received numerical predictions of residual impactor velocities as a function of initial impactor velocity.

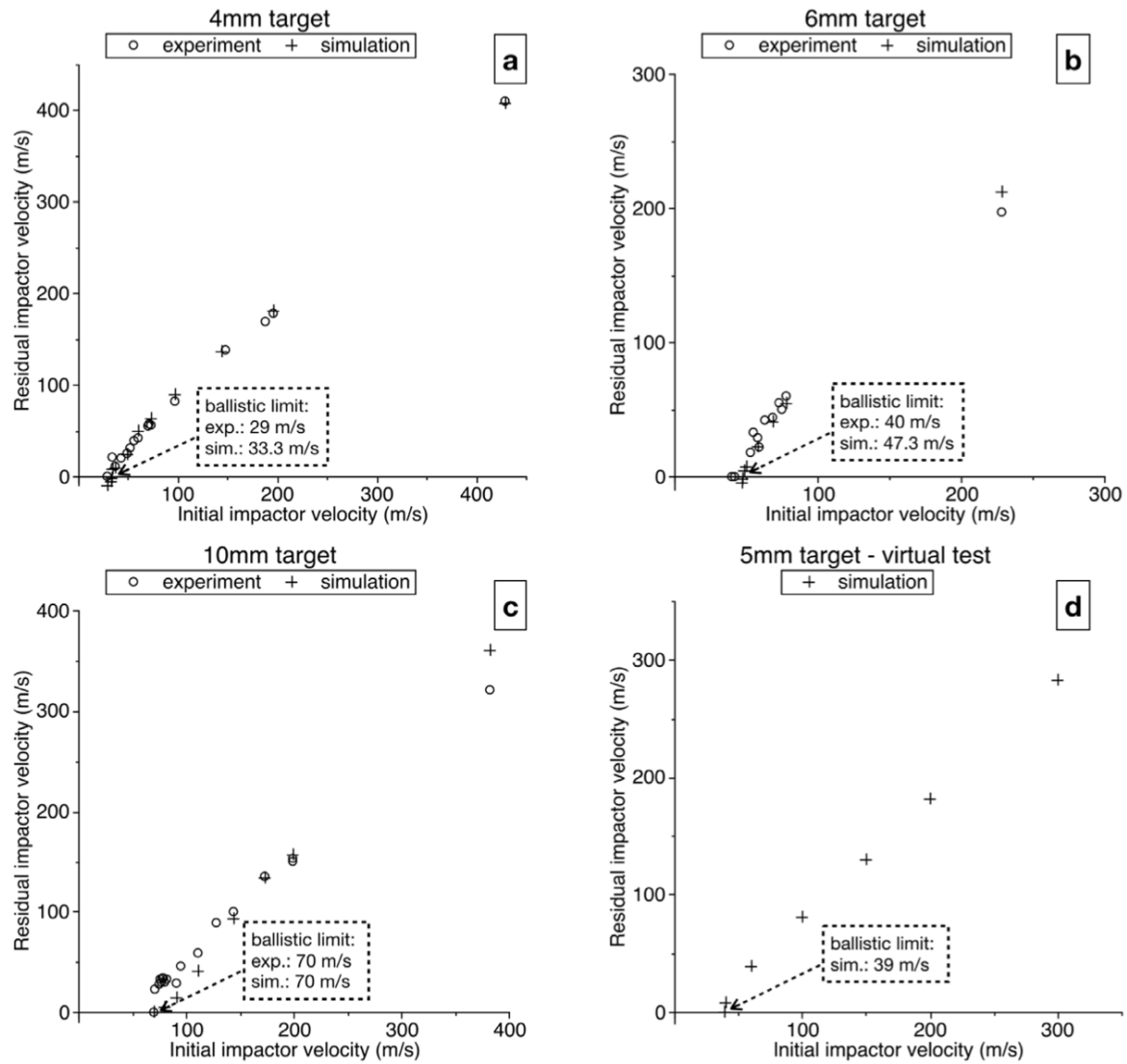


Fig. 11. Residual impactor velocities as a function of initial impactor velocity for the three experimentally tested PMMA plate thicknesses. d) gives the same dependency for a plate with 5mm thickness [31]

Figure 12 shows experimental and numerical fracture patterns for three different initial velocities for a 10mm thick PMMA plate.

A very close coincidence between the experimental measurements and numerical simulations utilizing the incubation time fracture criterion is the indication of the applicability of the presented approach for simulation of high-velocity interaction between impactors and quasibrittle targets. Once again it should be noted that the utilized model contains no "tuning" parameters. The model is using only experimental geometry, initial and boundary conditions, and material properties given in Table 4.

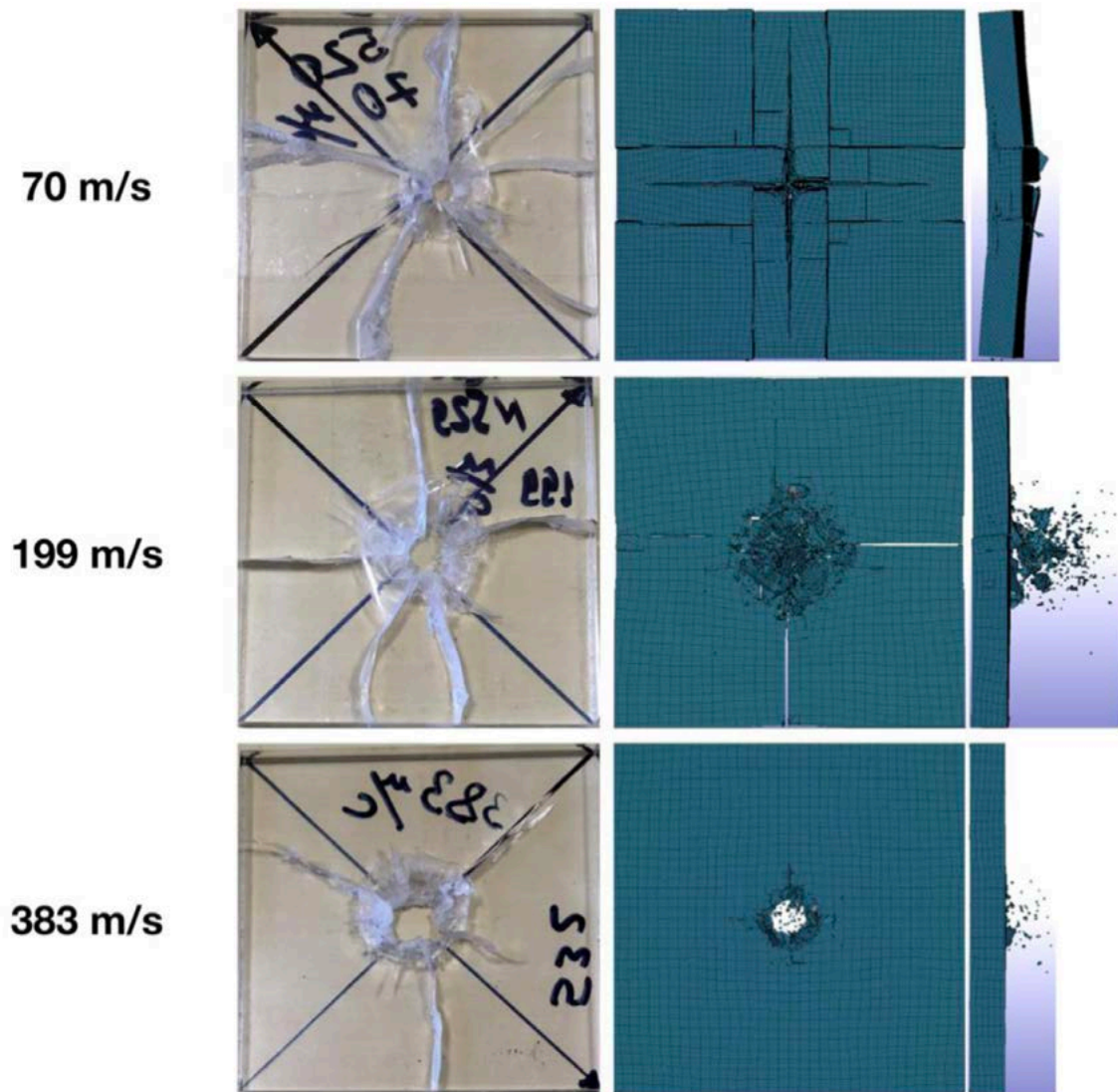


Fig. 12. Experimental and numerical fracture patterns for 10mm PMMA plates and three different initial impactor velocities [31]

11. Conclusions

The paper presented a review of available rupture criteria and numerical approaches for simulation of dynamic crack propagation and fracture of initially intact media. The incubation time approach for the prediction of quasibrittle dynamic fracture was discussed in better detail. Several examples of simulations including dynamic crack initiation, propagation, arrest, and reinitiation are presented. Examples of the incubation time approach utilized to simulate the evolution of brittle fracture in initially intact media were also presented. As vividly demonstrated, the incubation time approach, not incorporating any "tuning" parameters can reliably predict both the evolution of macroscopic cracks as well as the development of fracture zone in initially intact media loaded by high-energy impactors. Interconnection between crack velocity and stress intensity factor in the crack tip is discussed and results of simulations are presented. It is shown that the relation between the crack velocity and the stress intensity factor is not a material property, but also depends on experimental geometry, loading conditions, etc.

Acknowledgements. No external funding was received for this study.

References

- [1] Hopkinson J. *Original Papers*. Cambridge: Cambridge University Press; 1901.
- [2] Wallner H. Linienstrukturen an bruchflächen. *Zeitschrift für Physik*. 1938;114: 368-370.
- [3] Schardin H, Struth W. Hochfrequenzkinematographische untersuchung der bruchvorgänge in glas. *Glastechnische Berichte*. 1938;16: 219-230.
- [4] Wells AA, Post D. The dynamic stress distribution surrounding a running crack - A photoelastic analysis. *Proceedings of the Society for Experimental Stress Analysis*. 1958;16: 69-93.
- [5] Yoffe EH. The moving Griffith crack. *Philosophical Magazine*. 1951;42: 739-750.
- [6] Broberg KB. The propagation of a brittle crack. *Archiv für Physik*. 1960;18: 159-192.
- [7] Atkinson C, Eshelby JD. The flow of energy into the tip of a moving crack. *International Journal of Fracture*. 1968;4: 3-8.
- [8] Bradley WB, Kobayashi AS. An investigation of propagating crack by dynamic photoelasticity. *Experimental Mechanics*. 1970;10: 106-113.
- [9] Kobayashi AS, Wade BG, Bradley WB, Chiu ST. Crack branching in Homalite-100 plates. *Engineering Fracture Mechanics*. 1974;6: 81-92.
- [10] Dally JW. Dynamic photoelastic studies of fracture. *Experimental Mechanics*. 1979;19: 349-361.
- [11] Ravi-Chandar K, Knauss WG. An experimental investigation into dynamic fracture: I. Crack initiation and arrest. *International Journal of Fracture*. 1984;25: 247-262.
- [12] Ravi-Chandar K, Knauss WG. An experimental investigation into dynamic fracture: II. Microstructural aspects. *International Journal of Fracture*. 1984;26: 65-80.
- [13] Ravi-Chandar K, Knauss WG. An experimental investigation into dynamic fracture: III. On steady state crack propagation and crack branching. *International Journal of Fracture*. 1984;26: 141-154.
- [14] Ravi-Chandar K, Knauss WG. An experimental investigation into dynamic fracture: IV. On the interaction of stress waves with propagating cracks. *International Journal of Fracture*. 1984;26: 189-200.
- [15] Dally JW, Shukla A. Energy loss in Homalite-100 during crack propagation and arrest. *Engineering Fracture Mechanics*. 1980;13: 807-817.
- [16] Kalthoff JF. Fracture behavior under high rates of loading. *Engineering Fracture Mechanics*. 1986;23: 289-298.
- [17] Dally JW, Barker DB. Dynamic measurements of initiation toughness at high loading rate. *Experimental Mechanics*. 1988;28: 298-303.
- [18] Rosakis AJ, Zehnder AT. On dynamic fracture of structural metals. *International Journal of Fracture*. 1985;27: 169-186.
- [19] Freund LB. Crack propagation in an elastic solid subjected to general loading. I: Constant rate of extension. *Journal of Mechanics and Physics of Solids*. 1972;20: 129-140.
- [20] Freund LB. Crack propagation in an elastic solid subjected to general loading. II: Nonuniform rate of extension. *Journal of Mechanics and Physics of Solids*. 1972;20: 141-152.
- [21] Freund LB. Energy flux into the tip of an extending crack in an elastic solid. *Journal of Elasticity*. 1972;2: 341-349.
- [22] Kostrov BV. Unsteady propagation of longitudinal shear cracks. *Applied Mathematics and Mechanics*. 1966;30: 1241-1248.
- [23] Kostrov BV, Nikitin LV. Some general problems of mechanics of brittle fracture. *Archiwum Mechaniki Stosowanej*. 1970;22: 749-775.
- [24] Achenbach JD. Dynamic effects in brittle fracture. In: Nemat-Nasser S. (Ed.) *Mechanics today*. NY: Pergamon, Elmsford; 1974. p.1-57.
- [25] Willis JR. Equations of motion for propagating crack. *Mechanics and Physics of Fracture, The Metals Society of London*. 1975;1: 57-67.

- [26] Freund LB. *Dynamic fracture mechanics*. Cambridge: University Press; 1990.
- [27] Broberg KB. The near-tip field at high crack velocities. *International Journal of Fracture*. 1989;39: 1-13.
- [28] Owen DM, Zhuang S, Rosakis AS, Ravichandran G. Experimental Determination of Dynamic Crack Initiation and Propagation Fracture Toughness in Thin Aluminum Sheets. *International Journal of Fracture*. 1998;90: 153-174.
- [29] Morozov N, Petrov Y. *Dynamics of Fracture*. Berlin: Springer; 2000.
- [30] Petrov YV, Morozov NF. On the modeling of fracture of brittle solids. *Journal of Applied Mechanics*. 1994;61: 710-712.
- [31] Kazarinov NA, Bratov VA, Morozov NF, Petrov YV, Balandin VV, Iqbal MA, Gupta NK. Experimental and numerical analysis of PMMA impact fracture. *International Journal of Impact Engineering*. 2020;143: 103597.
- [32] Smirnov V, Petrov YV, Bratov V. Incubation time approach in rock fracture dynamics. *Science China Physics, Mechanics and Astronomy*. 2012;55(1): 78-85.
- [33] Bratov V. Incubation time fracture criterion for FEM simulations. *Acta Mechanica Sinica*. 2011;27(4): 541-549.
- [34] Kazarinov N, Bratov V, Petrov Y. Modelling dynamic propagation of a crack at quasistatic loading. *Doklady Physics*. 2014;59(2): 99-102.
- [35] Bratov V, Petrov Y, Utkin A. Transient near tip fields in crack dynamics. *Science China Physics Mechanics and Astronomy*. 2011;54(7): 1309-1318.
- [36] Bratov VA, Morozov NF, Petrov YV. Simulating the SMART1 orbiter impact on the Moon's surface. *Doklady Physics*. 2008;53(3): 152-155
- [37] Bratov V, Krivtsov A. Analysis of energy required for initiation of inclined crack under uniaxial compression and mixed loading. *Engineering Fracture Mechanics*. 2019;216: 106518.
- [38] Holmquist TJ, Templeton DW, Bishnoi KD. Constitutive modeling of aluminum nitride for large strain, high-strain rate, and high-pressure applications. *International Journal of Impact Engineering*. 2001;25(3): 211-231.
- [39] Tabiei A, Zhang W. Cohesive element approach for dynamic crack propagation: Artificial compliance and mesh dependency. *Engineering Fracture Mechanics*. 2017;180: 23-42.
- [40] Aubertin P, Réthoré J, De Borst R. Dynamic Crack Propagation Using a Combined Molecular Dynamics/Extended Finite Element Approach. *International Journal for Multiscale Computational Engineering*. 2010;8(2): 221-235.
- [41] Bleyer J, Roux-Langlois C, Molinari JF. Dynamic crack propagation with a variational phase-field model: limiting speed, crack branching and velocity-toughening mechanisms. *International Journal of Fracture*. 2017;204: 79-100.
- [42] Remmers J, de Borst R, Needleman A. The simulation of dynamic crack propagation using the cohesive segments method. *Journal of the Mechanics and Physics of Solids*. 2008;56(1): 70-92.
- [43] Grégoire D, Maigre H, Réthoré J, Combescure A. Dynamic crack propagation under mixed-mode loading – comparison between experiments and X- FEM simulations. *International Journal of Solids and Structures*. 2007;44: 6517-6534.
- [44] Liu ZL, Menouillard T, Belytschko T. An XFEM/Spectral element method for dynamic crack propagation. *International Journal of Fracture*. 2011;169: 183-198
- [45] Stolarska M, Chopp D, Moes N, Belytschko T. Modelling crack growth by level sets in the extended finite element method. *International Journal For Numerical Methods In Engineering*. 2001;51(8): 943-960.

- [46] Ghajari M, Iannucci L, Curtis P. A peridynamic material model for the analysis of dynamic crack propagation in orthotropic media. *Computer Methods in Applied Mechanics and Engineering*. 2014;276: 431-452.
- [47] Abraham FF, Brodbeck D, Rudge WE, Xu X. A molecular dynamics investigation of rapid fracture mechanics. *Journal of the Mechanics and Physics of Solids*. 1997;45(9): 1595-1619.
- [48] Aubertin P, Réthoré J, De Borst R. A molecular dynamics / extended finite element method for dynamic crack propagation. *International Journal for Numerical Methods in Engineering*. 2009;81(1): 72-88.
- [49] Petrov Y, Bratov V, Volkov G, Dolmatov E. Incubation Time Based Fracture Mechanics and Optimization of Energy Input in the Fracture Process of Rocks. In: Zhou Y, Zhao J. (Eds.) *Advances in Rock Dynamics and Applications*. NY: CRC Press; 2011; p.163-184.
- [50] Bratov V, Petrov Y Application of incubation time approach to simulate dynamic crack propagation. *International Journal of Fracture*. 2007;146: 53-60.
- [51] *ANSYS User's Guide*. Release 11.0. ANSYS Inc., Pennsylvania, USA; 2006.
- [52] Petrov YV, Morozov NF, Smirnov VI. Structural micromechanics approach in dynamics of fracture. *Fatigue and Fracture of Engineering Materials and Structures*. 2003;26: 363-372.
- [53] Berezkin AN, Krivosheev SI, Petrov YV, Utkin AA, Effect of Delayed Crack Nucleation under Threshold Pulse Loading. *Doklady Physics*. 2000;45(11): 617-619.
- [54] Fineberg J, Gross SP, Marder M, Swinney HL. Instability in Crack Propagation. *Physical Review*. 1992;45(10): 5146-5154.
- [55] Sharon E, Fineberg J. The Dynamics of Fast Fracture. *Advanced Engineering Materials*. 1999;1(2): 119-122.
- [56] Kazarinov N, Bratov V, Petrov Y. Simulation of dynamic crack propagation under quasistatic loading. *Applied Mechanics and Materials*. 2014;532: 337-341.
- [57] Broberg KB. The propagation of a brittle crack. *Arkiv för Fysik*. 1960;18: 159-192.
- [58] Barenblatt GI, Cherepanov GP. On the wedging of brittle bodies. *Journal of Applied Mathematics and Mechanics (PMM)*. 1960;24: 993-1014.
- [59] Craggs JW. On the propagation of a crack in an elastic-brittle material. *Journal of the Mechanics and Physics of Solids*. 1960;8: 66-75.
- [60] Kaplunov J, Prikazchikov DA. Asymptotic theory for Rayleigh and Rayleigh-type waves. *Advances in applied mechanics*. 2017;50: 1-106.
- [61] Kerkhof F. Wave fractographic investigation of brittle fracture dynamics. In: Sih GC. *Dynamic Crack Propagation*. Leyden; International Publishing; 1973. p.3-35.
- [62] Tian F, Tang X, Xu T, Yang J, Li L. Bifurcation criterion and the origin of limit crack velocity in dynamic brittle fracture. *International Journal of Fracture*. 2020;224: 117-131.
- [63] Griffith AA. The phenomena of rupture and flow in solids. *Philosophical Transactions of the Royal Society of London A*. 1920;221: 163-198.
- [64] Irwin GR. Fracture dynamics. In: *Fracturing of metals*. Cleveland, Ohio: ASM; 1948. p.147-166.
- [65] Neuber, H. *Kerbspannunglehre: Grundlagen für Genaue Spannungsrechnung*. Berlin: Springer; 1937.
- [66] Neuber H. *Theory of Notch Stresses: Principle for Exact Stress Calculations*. Edwards, Ann Arbor; 1946.
- [67] Novozhilov VV. About the necessary and sufficient brittle strength criterion. *Prikladnaya Matematika i Mekhanika*. 1969;33(2): 212-222.
- [68] Khan MK, Iqbal MA, Bratov V, Morozov NF, Gupta NK. An investigation of the ballistic performance of independent ceramic target. *Thin-Walled Structures*. 2020;154: 106784.

- [69] Rajesh P, Lakshmana R. Numerical Simulation of Ballistic Impact on Particulate Composite Target using Discrete Element Method:1-D and 2-D Models. *International Journal for Computational Methods in Engineering Science and Mechanics*. 2014;15: 9-16.
- [70] Meng S, Taddei L, Lebaal N, Roth S. Advances in ballistic penetrating impact simulations on thin structures using Smooth Particles Hydrodynamics: A state of the art. *Thin-Walled Structures*. 2021;159: 107206.
- [71] *European Space Agency. Impact landing ends SMART-1 mission to the Moon*. Available from: https://www.esa.int/Newsroom/Press_Releases/Impact_landing_ends_SMART-1_mission_to_the_Moon Accessed 11 May 2021.
- [72] *European Space Agency. Intense final hours for SMART-1*. Available from: https://www.esa.int/Science_Exploration/Space_Science/SMART-1/Intense_final_hours_for_SMART-1 Accessed 11 May 2021.